Aspirating Gas Detection – CFD Modelling Predicts Application Performance

Yun Jiang
Xtralis, Bentleigh East, Australia

Claudio Groppetti
Xtralis, Avon, MA, USA

Abstract

Historically gas detection has utilized a variety of detector types ranging from fixed point, single point aspirating, sequential multi-point aspirating or open path type. Recently an aspirating gas detection system was introduced as an accessory to a very early warning aspirating smoke detector (ASD). The new combination of aspirating smoke and gas detector (ASD-Gas) system utilizes the ASD pipe network to draw an air sample into the gas detector. This paper described CFD modelling for the prediction of temporal and spatial distributions of gases and vapours generated from liquid evaporation, gas leakage, and vehicle exhaust emission. The results demonstrate the viability of this method as an alternative to conventional gas detection as well as providing additional insight regarding the proper design and application of this approach.

Keywords: Aspirating, gas detection, CFD modelling

Introduction

Very early warning Aspirating Smoke Detection has been widely adopted as a powerful fire detection technology due to its ability to detect fires in their incipient stage. This technology provides valuable time to investigate and mitigate the situation before fire escalation occurs and causes significant damage. Usage of fire detection systems is typically driven by codes and standards for life safety, building and process protection. Gas detection on the other hand has far fewer codes and standards to follow and is typically used based on risk assessment. Integrating both detection systems into one package delivers a unique and cost-effective solution with significant advantages, including; improved area coverage, continuous monitoring, and the ability to condition and process the air stream which improves the detector's reliability and extends its life.

An ASD-Gas detection system consists of an ASD system with gas detector(s) attached on the sampling pipe(s), illustrated in **Fehler!**

Verweisquelle konnte nicht gefunden werden.. Gas sampling positions are flexible, from Option 1 through single hole, Option 2 multiple holes on a pipe branch, to Option 3 all holes of the ASD smoke detector on its exhaust pipe.

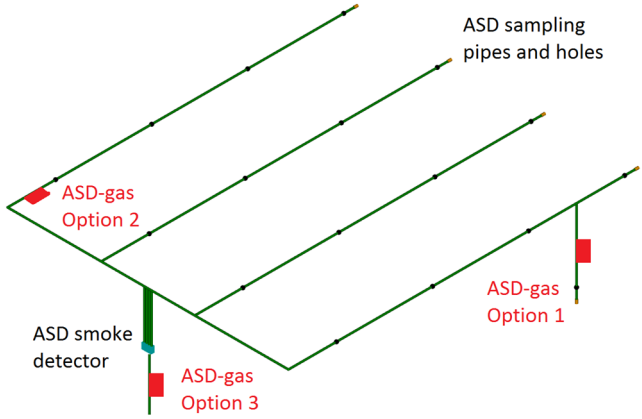

Figure 1. ASD-gas detection.

There are dozens of gas sensor types available for the ASD-Gas system ranging from toxic to flammable gases. The gas detection system has been characterised using several parameters including; flowrate, pressure, temperature, humidity, gas attenuations by filter and pipe network, etc. Its detection performance is dependent on the distribution of targeted gases and design of the gas sampling network. CFD modelling by Fire Dynamics Simulator (FDS)[1] was utilised to better understand gas distribution and predict detection performance in several different leak scenarios.

Section 1 – Gas leakage and liquid evaporation

For the purpose of this study, gas leaks were simulated as jet leaks for the lighter gases and evaporation from liquid pools for the heavier gases. Basic properties of the gases and liquids studied are listed in Table 1.

Table 1. Species under study.

Species	Formula	Mol. Wt.	Spec. Gravity (Water=1)	Temp-boil (°C)	Spec. Mol. Gravity (Air=1)
Hydrogen	H_2	2.02		-252.9	0.07
Methane	CH_4	16.04		-161.5	0.55
Methanol	CH_2OH	32.04	0.793	64.5	1.11
Ethanol	C_2H_5OH	46.07	07.89	78.5	1.59
N-heptane	C_7H_{16}	100.2	0.688	98.5	3.46

CFD modelling was performed using two sizes of rooms, small (10x10x3 m) and medium (18x28x6 m), at air velocities of 0, 0.5, and 1m/s (0, 6 and 12 ACH respectively). Table 2 shows ventilation schemes studied.

Table 2. Ventilation scheme.

Description	Supply Register	Exhaust Register
L-L (low-low)	Floor level (fan)	Floor level (opening)
L-H (low-high)	Floor level (opening)	Ceiling level (fan)
H-L (high-low	Ceiling level (fan)	Floor level (opening)

Gas phase concentrations were monitored at various locations, as shown in Table 3.

Table 3. Sampling location, coverage and spaces

Description	Sample Location	Coverage or Spacing	Label
Ceiling	At ceiling	50m^2 & 83m^2 per hole for small and medium rooms	ASD-G_C
Vertical	At centre of room	0.1, 0.3, 1m to ceiling	ASD-G_V
Wall	On the walls	0.1, 0.3, 1m to ceiling	ASD-G_W

Gas leakage and dispersion

Gas leakage was assessed under leakage rates of 0.3 and 0.5 mol/s in the small room and at 1 and 2 mol/s in the medium room. It was found that the two lighter gases have similar behaviour in dispersion, rising up to the ceiling directly, illustrated in **Fehler! Verweisquelle konnte nicht gefunden werden.**. They also have similar trends in gas distribution. Table 4 shows major results of Hydrogen and Methane distributions in the small and medium rooms respectively.

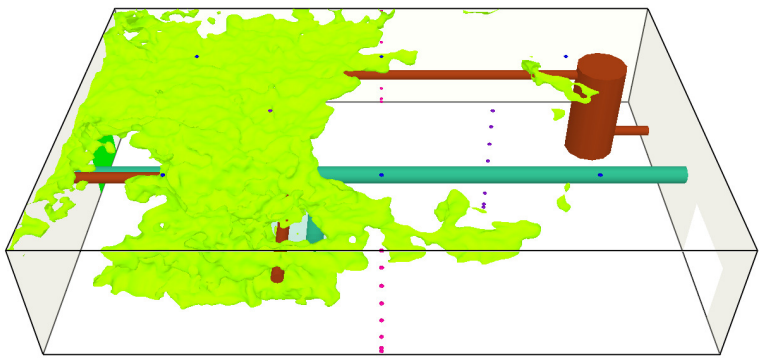

Figure 2. H_2 dispersion in the medium room.

In both small and medium rooms, gas concentrations were proportional to the release rates in the still environment. As the ventilation increased, gas concentrations decreased. The still environment represents the worst case for potential ignition and explosion. Among the ventilation schemes, the L-H scheme was most effective in reducing the gas concentration as the exhaust vent was located close to the ceiling.

Table 4. Gas distribution and detection in the rooms.

Leak rate (mol/s)	Vent Scheme	Flow Rate (ACH)	Gas concentration				Detection performance				
			Under ceiling			0.1m H	ASD-G_C			ASD-G_V	ASD-G_W
			Max (%LFL)	L-50 (s)	L-100 (s)	Max (%LFL)	Max (%LFL)	L-50 (s)	L-100 (s)	Max (%LFL)	Max (%LFL)
Hydrogen in the small room											
0.3		0	88.5	500	>1200	51.2	87.8	560	>1200	66.7	68.8
0.5		0	146.1	235	745	88.9	144.0	270	770	114.2	116.4
0.3	L-L	6	77.9	550	>1800	18.9	76.7	645	>1800	49.5	48.6
0.3	L-L	12	70.1	635	>1800	14.7	65.1	870	>1800	32.8	36.2
0.5	L-L	6	89.9	315	>1800	11.6	82.5	380	>1800	41.3	44.5
0.5	L-L	12	87.7	270	>1800	15.5	85.8	325	>1800	42.7	42.8
0.5	L-H	6	75.1	340	>1800	11.6	72.0	340	>1800	34.4	35.2
0.5	H-L	6	99.7	260	>1800	35.1	96.3	290	>1800	59.2	58.8
Methane in the medium room											
1		0	56.1	915	>1000	0	43.4	>1000		16.7	17.1
2		0	91.1	115	>1000	0.9	71.7	525	>1000	32.9	33.3
1	L-L	6	46.7	>1800		6.6	39.2	>1800		21.2	21.8
2	L-L	6	77.1	335	>1800	10.5	66.2	865	>1800	38.2	36.8
2	L-L	12	80.5	245	>1800	11.2	61.3	930	>1800	29.9	30.4
2	L-H	6	66.2	1110	>1800	6.2	45.8	>1800		16.9	19.2

Note: L-50 and L-100, alarm times at 50 and 100%LFLs

In the small room, a single sampling point at ceiling height indicated the highest concentration. Comparing to it, ASD-G_C option has differences within 10 % in concentration and 4 minutes in alarm time, due to dilution effect. In the medium room, the ASD-G_C option read 15-30 % lower than the single point due to heavier dilution from the 6 sampling holes. By adjusting alarm thresholds to compensate for dilution similar detection performance to the point detector can be achieved.

Liquid evaporation and dispersion

Evaporation rates of the liquids were calculated using surface areas of 10, 25 and 100 m^2. The liquids were exposed to 40 °C airflow with velocity from 0.1 to 1 m/s across the surface. The modelled evaporation rates were then used to specify gas release rates in the study of dispersion in the rooms. Evaporation rates from a 25 m^2 pool and under

0.5 m/s airflow for Methanol, Ethanol and N-heptane were 2.91, 1.39, and 0.26 g/s respectively.

The vapours from the evaporated liquids remain near the floor under all ventilation conditions due to their heavier mol. specific gravities. Figure 3 shows maximum gas concentrations modelled at 0.1 m above the floor in the small room for Methanol (ME), Ethanol (ET) and N-heptane (HE).

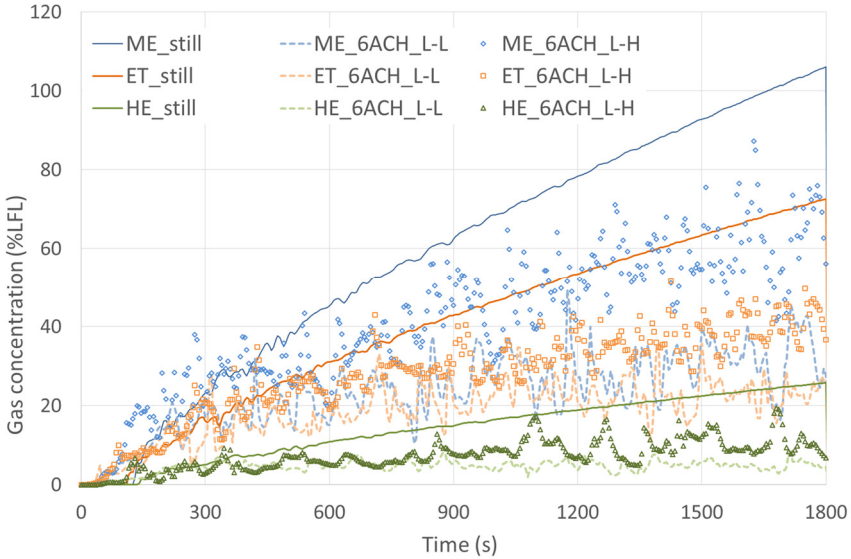

Figure 3. Maximum gas concentrations from 25 m^2 pool evaporation.

The highest & lowest concentrations are obtained from Methanol & N-heptane due to their highest & lowest evaporation rates per unit of area. Contrary to the lighter gases, the highest gas concentrations of these vapours are predicted at 0.1 m height using the L-H scheme while the L-L scheme generates the lowest peak due to its strongest extraction.

Detection options

To optimize detection of gases sampling should take place in the spaces with the highest concentrations expected; close to the ceiling and floor for lighter and heavier gases respectively. The options that spread sampling points vertically (ASD-G_V and ASD-G_W) were not effective in detection of layered gas and vapours, as shown in Table *4* for example. Sampling at ceiling ASD-G_C option is effective in detection of lighter gases. As the area being monitored or airflow increases potential dilution effect should be compensated for by either limiting the number of sampling points per detector or lowering the alarm thresholds. Sampling height also plays a critical role for the detection of heavier vapours. When the sampling height increases from

0.1 m to 0.3 and 0.5 m, Methanol concentration drops 74 and 95 % in still air, 10 and 24 % under 6ACH ventilation respectively in the small room. Actual sample point height and alarm threshold setting must take into account both specific gravity of the vapour and ventilation conditions within the space.

Section 2 – CO detection in car parks

Carbon monoxide monitoring is required in car parks by a number of international codes with specified coverage varying from 200 m^2 in Spain (UNE 100166), 400 m^2 in Germany (VDI 2053) to 1250 m^2 in Australia (AS 1668) for instance. As the CO concentration monitored by CO detectors reaches pre-set thresholds, demand-control ventilation systems are activated to extract vehicle emissions. Air quality is therefore maintained for human health. CFD modelling was performed to determine optimum sample point placement in ASD-Gas system to achieve a performance equivalent to or better than the point type CO detector.

Modelling of CO distribution from car exhaust

CFD modelling was conducted in a car park environment with ceiling height of 3.2 m. The profiles of exhaust from a passenger car (under idle and low speed moving conditions) was adopted from EPA data [2]. The emission was simplified as consistent CO release rate of 4.26 g/min and 5 kW heat output.

Point type CO detector was installed at breathing height, between 0.9 and 2.5 m as specified by AS 1668. The ASD-Gas CO detection sampling points were located at the ceiling as per requirements of smoke detection. ASD-Gas CO detection with multiple sampling points was assessed using CFD modelling.

The dispersion of CO within a space occurs easily due to its molecular weight being similar to air. Assisted by the heat in the exhaust, CO movement becomes directional, rising up and then spreading under the ceiling, similar to smoke movement from a fire. Shown in Figure 4 are results from CO released from 4 vehicles while stopped in a still air environment. CO concentrations were from point detector at different heights and different coverage areas for the ASD-Gas CO detector.

From the ceiling (3.2 m) to 2.5 m high, CO concentration drops significantly, by approximately 50 to 75 % lower. ASD-Gas CO detectors read lower levels than the points under the ceiling. This can be attributed to dilution effect from multiple holes. Compared to point detector mounted at breathing height of 2.5 m, ASD-Gas systems have higher concentration and quicker response, as shown in Figure *4*.

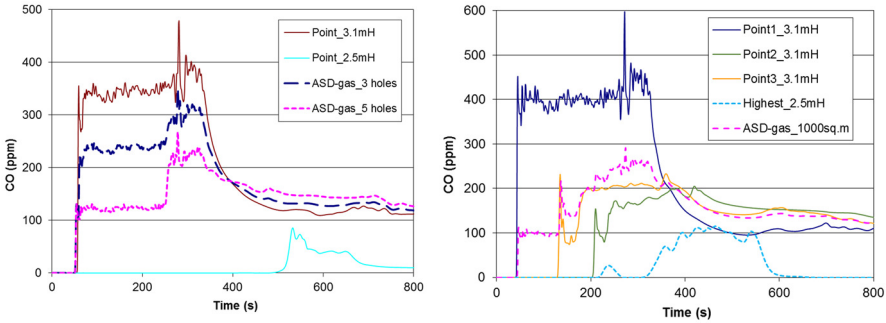

(a) 100 m^2 coverage (b) 1000 m^2 coverage

Figure 4. CO concentrations at various height and coverage.

Various detector coverage and ventilation zones were studied in the modelling. It's confirmed that ASD-Gas CO detection sampling under the ceiling can achieve better detection performance than point CO detector mounted at breathing height. Table 5 shows recommended ASD-Gas CO sampling coverage & options to match with point type CO detector performance.

Table 5. Recommendations on ASD-Gas CO detection coverage.

Point detection coverage (m^2)	ASD-Gas detector coverage (m^2)	Sampling option
1000-1300	Same as point detector	Option 3
400-500	400-800	Option 2 & 3
100-200	Up to 500	Option 2

Experimental validation

Validation tests were conducted in a 4 m high loading area of a car park. An ASD-Gas system was installed to monitor a loading bay with floor area of approximate 100 m^2. A CO gas sensor was attached on its exhaust pipe of the ASD as shown in Option 3 (**Fehler! Verweisquelle konnte nicht gefunden werden.**). Due to installation limitations a CO point detector was installed at the centre of the space at ceiling height. CO concentrations were recorded in the ASD-Gas and point type CO detectors spanning several months. Figure 5 shows measured concentrations for one-week of normal operation.

The ASD-Gas and point type CO detection systems have similar long-term & transient changes and magnitudes of CO concentration making them basically equivalent in this configuration. CO concentrations at the ceiling are much higher than those measured in the breathing zone. Combining this information with the data shown in Figure 4 it can be

implied that the ASD-Gas system can deliver improved detection with greater coverage.

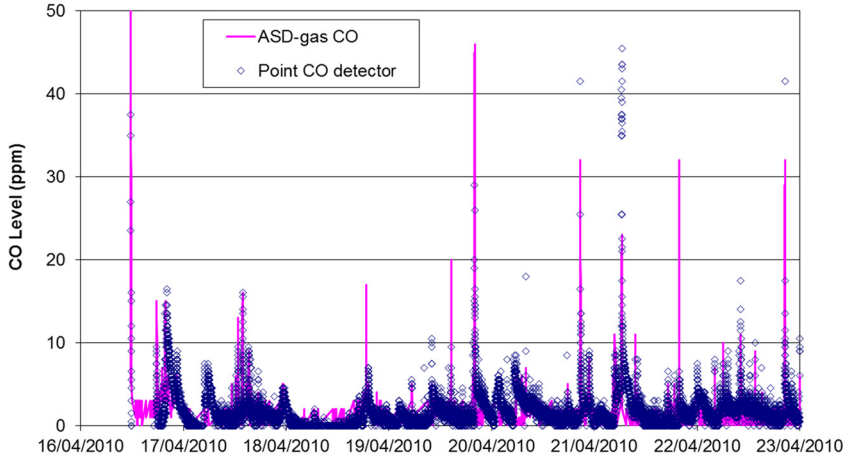

Figure 5. CO values recorded over one week.

Section 3 – CO & NO_2 detections in a road tunnel

For the protection of a proposed freeway tunnel in the North America, an integrated ASD-Gas system was designed to provide both fire and gas detections. An ASD-Gas system was proposed to replace point type CO and NO_2 detectors. CFD modelling was performed to assess ASD fire detection performance under fire scenarios tested in a previous FPRF road tunnel fire detection project [3]. Additional modelling was conducted to study distributions of CO and NO_2 released from gasoline and diesel engine vehicles. EPA 2000 data [2] for a passenger car unit (PCU) and a heavy goods vehicle (HGV) were used for the CO and NO_2 release rates, as 20.9g/mile and 8.6g/mile respectively. The air movement caused by traffic was modelled as airflow introduced from one end of the tunnel, at velocities of 0m/s (still), 0.8 m/s (weak airflow), 3 m/s (normal operation) and 5 m/s (strong airflow).

The ASD fire detector covered 100 m length of the tunnel and sampled at the ceiling (5.4 m high). Every 50 m section was covered by 2 parallel sampling pipes separated in 4.5 m. ASD-Gas detector used Option 2 (1 pipe with 6 holes) and Option 3 (all 24 holes) sampling methods as illustrated in Figure 1. Point type CO and NO_2 detectors were spaced every 91.5 m (300 ft) as per NFPA 502. The mounting heights were at breathing height (1.8 m), halfway (2.7 m) and at the ceiling.

Table 6 shows modelled detection performances of ASD-Gas system and the point type detector outputs averaged over 30 seconds.

Table 6. Modelling results of gas detections.

Gas	Airflow (m/s)	ASD-Gas (ppm)		Point detector (ppm)	
		All ASD holes	1 ASD pipe	@1.8mH	Under ceiling
CO	0	205	212	2.4	200
	0.8	80	101	80	105
	3	21	28	30	30
	5	21	26	50	30
NO_2	0	34	36	3	47
	0.8	6	16	21	26
	3	2	2	5	5

Under low air velocities, including still (simulating stopped traffic) and 0.8 m/s (traffic queueing), CO concentration in the tunnel would exceed 70 ppm, a threshold set by the consultant and end-user. Both the ASD-Gas system options can detect CO emission effectively under low air flows. As the air flow increased, caused by higher traffic speed, CO emissions are diluted by the air flow and are significantly reduced.

All the ASD-Gas system options and point type CO detectors provide similar detection performance.

Nitrogen dioxide was released from small portion of diesel vehicles (18 %) in the modelling. High gas concentration was formed locally under low ventilation, and ASD-Gas detections had readings slightly lower than the point detector under ceiling but higher than the point detector at 1.8 m. Under higher air velocity dispersion of NO_2 becomes uniform in height and difference among the detections becomes smaller. In-situ tests should be conducted for validation and determination on threshold.

Conclusions

CFD modelling has demonstrated that ASD-Gas detection technology can provide a viable alternative to point type gas detectors and is a cost-effective, reliable & flexible smoke and gas detection solution. Successful deployment is dependent upon thorough understanding applicable codes and standards and the risk assessment. Understanding the properties of the gases and vapours to be detected along with all environmental conditions is critical to successful in real applications.

References

[1] K.B. McGrattan, B. Klein, S. Hostikka, G.P. Forney, G.P., "*Fire Dynamics Simulator (Version 5) User's Guide*", NIST Special

Publication 1019-5, National Institute of Standards and Technology, Gaithersburg, MD, 2007

[2] EPA, "*Idling vehicle emissions for passenger cars, light-duty trucks, and heavy-duty trucks*", Emission Facts, EPA, Oct. 2008.

[3] Z.G. Liu, A. Kashef, G. Lougheed, G. Crampton, D.T. Gottuk, "*Summary of International Road Tunnel Fire Detection Research Project – Phase II*", The Fire Protection Research Foundation, MA, USA, 2008